High-resolution nitrogen stable isotope sclerochronology of bivalve shell carbonate-bound organics

David P. Gillikin, Anne Lorrain, Aurélie Jolivet, Zita Kelemen, Laurent Chauvaud, Steven Bouillon

High-resolution nitrogen stable isotope sclerochronology of bivalve shell carbonate-bound organics

David P. Gillikin[1], Anne Lorrain[2], Aurélie Jolivet[2,3], Zita Kelemen[4], Laurent Chauvaud[2] and Steven Bouillon[4]

Abstract.

Nitrogen stable isotope ratios ($\delta^{15}N$) of organic material have successfully been used to track food web dynamics, nitrogen baselines, pollution, and nitrogen cycling. Extending the $\delta^{15}N$ record back in time has not been straightforward due to a lack of suitable substrates in which $\delta^{15}N$ records are faithfully preserved, thus sparking interest in utilizing skeletal carbonate-bound organic matter (CBOM) in mollusks, corals, and foraminifera. Here we test if calcite *Pecten maximus* shells from the Bay of Brest and the French continental shelf can be used as an archive of $\delta^{15}N$ values over a large environmental gradient and at a high temporal resolution (approximately weekly). Bulk CBOM $\delta^{15}N$ values from the growing tip of shells collected over a large nitrogen isotope gradient were strongly correlated with adductor muscle tissue $\delta^{15}N$ values (R^2=0.99, n= 6, p<0.0001). We were able to achieve weekly resolution (on average) over the growing season from sclerochronological profiles of three shells, which showed large seasonal variations up to 3.4‰. However, there were also large inter-specimen differences (up to 2.5‰) between shells growing at the same time and location. Generally, high-resolution shell $\delta^{15}N$ data follow soft-tissue $\delta^{15}N$ values, but soft-tissues integrate more time, hence soft-tissue data are more time-averaged and smoothed. Museum-archived shells from the 1950s, 1965, and 1970s do not show a large difference in $\delta^{15}N$ values through time despite expected increasing N loading to the Bay over this time, which could be due to anthropogenic N sources with contrasting values. Compiling shell CBOM $\delta^{15}N$ data from several studies suggests that the offset between soft-tissue and shell $\delta^{15}N$ values ($\Delta_{tissue\text{-}shell}$) differs between calcite and aragonite shells. We hypothesize that this difference is caused by differences in amino acids used in constructing the different minerals, which should be specific to the $CaCO_3$ polymorph being constructed. Future work should use compound specific isotope analyses (CSIA) to test this hypothesis, and to

47 determine whether certain amino acids could specifically track N sources or possibly identify
48 amino acids that are more resistant to diagenesis in fossil shells. In conclusion, bivalve shell
49 CBOM $\delta^{15}N$ values can be used in a similar manner to soft-tissue $\delta^{15}N$ values, and can track
50 various biogeochemical events at a very high-resolution.
51

1.0 Introduction

Nitrogen stable isotope signatures ($\delta^{15}N$) of organic matter are a powerful tool for studying food webs and tracking nitrogen dynamics in terrestrial and aquatic systems (Fry 1988; Cabana and Rasmussen 1996; Cole et al., 2011). Nitrogen in consumers is usually enriched in ^{15}N relative to their diet, typically by +2‰ to +4‰, or on average 3.4‰, which allows estimations of trophic positions of consumers relative to the base of the food web (De Niro and Epstein, 1981; Minigawa and Wada, 1984; Vander Zanden and Rasmussen 2001; Post 2002; Caut et al. 2009). It can however be difficult to estimate the isotopic composition of N sources at the base of the food web (isotopic baseline) since ecosystem biogeochemistry is dynamic and multiple nutrient sources available to phytoplankton can have distinct stable isotope signatures that vary temporally and spatially (McMahon et al. 2013). Bivalve soft-tissues have been proposed as good proxies of this isotopic baseline as they are sessile and integrate this variability (Jennings and Warr 2003, Vokhshoori and McCarthy 2014). Natural variations in $\delta^{15}N$ values of particulate N caused, for example, by upwelling (e.g., Mollier-Vogel et al. 2012) could thus be preserved in tissues, potentially serving as an upwelling / El Niño Southern Oscillation proxy in certain locations. In addition, $\delta^{15}N$ values of organics can be used as a wastewater pollution indicator (e.g., Costanzo et al 2005). Processed wastewaters are ^{15}N enriched, with $\delta^{15}N$ values of particulate N typically around +15‰ (Heaton, 1986), but much higher values have been recorded (e.g., Schlacher et al., 2007; Marwick et al., 2014; see Bouillon et al., 2012, for a review).

Extending organic $\delta^{15}N$ records back through time to develop isotopic baselines, or gather data on past pollution events, is challenging. Sediment $\delta^{15}N$ records can be used to track relative

changes, but sediment trap and surface sedimentary $\delta^{15}N$ values suggest alteration during early burial, cautioning against the use of sediment cores for reconstructing isotope baselines (reviewed in Robinson et al., 2012). Although there are excellent archives of preserved organic material in museums (e.g., animal soft-tissues), the effect of long-term preservation in formalin and/ or ethanol are not well characterized. Delong and Thorp (2009) recorded a -0.2 ‰ shift in freshwater mussel tissue $\delta^{15}N$ values after 12 months in ethanol. On the other hand, Carabel et al. (2009) reported a positive shift in $\delta^{15}N$ values of bivalve tissues of about +1 ‰ after storage in ethanol for two years. While these are not large effects considering the strong ^{15}N enrichment associated with anthropogenic N loading, it is not clear if longer time periods would result in larger isotopic shifts. For example, Versteegh et al. (2011) found more than a 5‰ difference in shell organic $\delta^{15}N$ values between shells stored dry and shells stored in ethanol for 73 years. Clearly, dry stored specimens would be the safer option for extending $\delta^{15}N$ data back in time. Typically, shells are stored dry in museum collections making them ideal archives for reconstructing past $\delta^{15}N$ values. Moreover, pristine unaltered fossils may also provide insights into the nitrogen cycle into the geological past (e.g., O'Donnell et al., 2003, 2007).

The study of nitrogen isotopes in carbonate bound organics has recently received renewed attention. Studies investigating N in carbonate bound organics in foraminifera (Ren et al., 2012a,b), corals (Marion et al. 2005; Williams and Grottoli, 2010; Yamazaki et al., 2011a, b, 2013; Wang et al., 2015), fish otoliths (Vandermyde and Whitledge, 2008; Rowell et al, 2010; Grønkjær et al., 2013), and bivalves (O'Donnell et al., 2007; Carmichael et al., 2008; Watanabe et al., 2009; Kovacs et al., 2010; Versteegh et al., 2011; Dreier et al., 2012; Graniero et al., 2016) have been increasing. Continuous long-term (>150 years) N isotope records have been developed

98 from coral skeletons (Erler et al., 2015), and foraminiferal N isotope records have been extended
99 back 30 Ka suggesting lower N fixation in the Atlantic during the last ice age (Ren et al. 2009),
100 both illustrating the power of this technique. Bivalves have a global distribution in many
101 environments, generally withstand pollution, are common, and are not mobile over large
102 distances allowing for spatial reconstructions. In addition, the dense 'closed' shells of bivalves
103 (Marin et al., 2007) exclude foreign organic material and make them relative diagenically
104 resistant (*c.f.*, Engel et al., 1994). Nevertheless, both corals and mollusk shells have been shown
105 to maintain their carbonate bound organics for hundreds to thousands of years (Engel et al 1994;
106 Ingalls et al., 2003). Therefore, similar to corals and foraminifera, bivalve shell carbonate is a
107 suitable structure to preserve high-resolution carbonate bound N.
108
109 As previously noted, bivalves are also a good substrate to target for N isotope studies because
110 they are low-level consumers and therefore record baseline $\delta^{15}N$ values (Jennings and Warr
111 2003). Finally, bivalves can be long-lived and have high growth rates allowing both high-
112 resolution environmental reconstruction (down to daily) and provide records extending back in
113 time (e.g., *Arctica islandica* shell chronologies have been extended back more than 1300 years;
114 Butler et al., 2013).
115
116 Although bivalve shells have higher %N than corals and foraminifera, they typically have only a
117 few percent organic matter bound within the carbonate (typically 1 to 5% organic matter; Marin
118 and Luquet 2004). This presents analytical challenges when determining such small amounts of
119 nitrogen in a large carbonate matrix, especially in a sclerochronological context. To circumvent
120 this problem, several studies have removed the carbonate via acidification (e.g., Carmichael et

al., 2008; Watanabe et al., 2009; Kovacs et al., 2010). However, several studies have shown that acidifying organic matter with high $CaCO_3$ content alters the $\delta^{15}N$ value (Jacob et al., 2005; Ng et al., 2007; Mateo et al., 2008; Serrano et al., 2008), likely because acidification removes all or part of the acid soluble N, leading to analysis of an unknown part of the bulk organic N. This has prompted other groups to directly combust the bulk shell to release the entire organic N pool, with good results (e.g., Vandermyde and Whitledge, 2008; Rowell et al, 2010; Versteegh et al., 2011; Graniero et al., 2016).

The aims of this study are 1) illustrate that low %N samples can be accurately measured on a standard elemental analyzer - isotope ratio mass spectrometer (EA-IRMS) configuration, 2) determine if bivalve shells can be used as an archive of $\delta^{15}N$ values, providing the same or parallel information as soft-tissues, and 3) determine if shells can provide an ultra-high-resolution $\delta^{15}N$ record (i.e., at a daily or weekly resolution).

2.0 Materials and Methods

2.1 Shell collection

This study presents data from three sets of *Pecten maximus* shell samples collected from the French coast: shells collected along a depth gradient in 2008, shells from the Bay of Brest collected in 2000, and three archived shells collected from the Bay over the past century. Shells were collected along a transect from the Bay of Brest, France (40 m depth, 4° 40’ W, 48° 18’ N), to the edge of the continental shelf (220 m depth, 8° 15’ W, 48° 12’ N) in 2008 (Fig 1; shell collection details and other data are provided in Nerot et al., 2012). Six shells from different depths (one per depth at 40, 78, 120, 140, 153, and 190 m) were analyzed along their ventral

144 margin covering the most recent one to five years of growth. Soft-tissue $\delta^{15}N$ values from the
145 adductor muscle (including those from the shells analyzed in this study) are from Nerot et al.
146 (2012) and range from 2.0 to 10.4‰ (n = 95). Three additional shells collected in the year 2000
147 from 30 m depth in the Bay were analyzed over their last year of growth with a resolution of 2 to
148 29 days per sample (average = 7.4 ± 6.4 days, median = 5 days). Monthly soft-tissue $\delta^{15}N$ values
149 from the adductor mussel and digestive gland collected over the 2000 calendar year are taken
150 from Lorrain et al. (2002) and represent average and standard deviations of five individuals all
151 collected at the same time and site as the shells. Shells were selected from those collected on
152 December 14, 2000; the last collection date of the Lorrain et al. (2002) study. Finally, archived
153 shells from the 1950s, 1965 and 1970s (one shell per time period, collected in the Bay; stored dry
154 without tissues, each covering about four years of growth) were also analyzed.
155
156 *2.2 Shell cleaning and sampling*
157 *Pecten maximus* produce dense, non-porous shells of foliated calcite microstructure without
158 pockets or chalky layers. Shell exteriors were scrubbed with a hard brush and cleaned with a
159 weak acid (acetic) for a few seconds to remove any extraneous particles and the periostracum
160 and to expose the underlying carbonate. Carbonate powder was milled from the exterior of the
161 cleaned shell surface following the daily growth striae this species produces using a hand held
162 drill. These striae, along with the known date of collection, allowed an absolute chronology to be
163 developed by counting back from the collection date (see Chauvaud et al., 1998; Lorrain et al.,
164 2004; Gillikin et al., 2008 as examples). Milling followed the striae along the curve of the shell,
165 only sampling the bottom of the rays (Fig 2). Care was taken to only sample the outer shell layer.
166 This sampling produced about 5 mg (5.47 ± 0.56 mg) of calcite powder, corresponding to ~5 µg

N (see Results) and resulting in a peak area of 8.5 ± 2.8 Volt-seconds (Vs) on the IRMS (equivalent to an amplitude of ~200 mV on mass 28). While the elemental analyzer can easily accommodate 40 mg, the small sample size was necessary to reduce time averaging required in a sclerochronological study. To double-check the reproducibility of this method, we resampled one of the shells collected in the year 2000 (shell B). Samples were milled between the samples taken during the first sampling, and were analyzed on a different date. These can be considered replicates, but also will contain real differences as they are effectively different samples and represent different time. Furthermore, an additional shell was used to test reproducibility. A larger section of this shell was milled and homogenized, from this, 7 samples were analyzed and were highly reproducible ($\delta^{15}N = 8.98 \pm 0.27$ ‰; $\%N = 0.07 \pm 0.002\%$).

As noted earlier, bivalves produce dense non-porous skeletons and therefore likely do not require the aggressive oxidative cleaning required for corals and foraminifera. In contrast, porous coral skeletons are known to contain foreign organic N from endolithic algae and fungi (Bentis et al., 2000) as well as humic acids (Susic et al., 1991), which can alter carbonate bound organic $\delta^{15}N$ values therefore necessitating an oxidative cleaning step (Erler et al., 2016). In addition to thin porous skeletons, foraminifera also have empty internal chambers, which can fill with sediments, also necessitating aggressive cleaning procedures (Ren et al., 2009). Bivalve shell organics on the other hand can be considered a "closed system" (Marin et al., 2007). In addition, foliated calcite bivalve shell microstructure is typically rather compact (in the absence of pockets or chalky layers such as in oysters) and is probably rather diagenetically stable, especially when compared with porous foraminifera or corals. We tested this hypothesis on another shell by analyzing growth lines from half the shell cleaned as mentioned above, and half the shell soaked

190 in a strong sodium hypochlorite solution (reagent grade, 10–15%) for 24 hours. Four samples
191 were milled from each half of the shell taking care to match timelines across shell halves (each
192 sequential sample moved forward in time). Differences between bleached and unbleached halves
193 ranged from 0.04 to 0.88 ‰ (Fig. 3). A paired T-test showed there is no statistical difference
194 between the bleached and unbleached halves ($p = 0.31$), and that the mean difference (0.34 ‰) is
195 less than expected analytical precision (0.5 ‰, see further). Moreover, both the bleached and
196 unbleached halves both show a decrease in $\delta^{15}N$ values along the shell (though time). The small
197 differences between the bleached and unbleached halves likely represent variable loss of acid
198 soluble N along the shell.
199
200 *2.3 Analytical methods and validation*
201 To test if our IRMS was capable of analyzing low N samples, various masses of the IAEA-N1
202 standard (ammonium sulfate; $\delta^{15}N = 0.4 \pm 0.2$‰) were analyzed. To facilitate preparing
203 standards with very low amounts of N, finely powdered IAEA-N1 material was mixed with
204 IAEA-CH6 sucrose standard (which does not contain N). Standards were weighed into standard
205 tin cups and combusted on a standard EA-IRMS setup (Thermo Flash HT with a Costech zero
206 blank autosampler, coupled to a Thermo DeltaV Advantage via a Thermo ConFlo IV) at KU
207 Leuven, Belgium. No modifications were made to the standard operating procedure (e.g.,
208 combustion column and reduction column at 1070 °C and 640 °C respectfully; an inline CO_2 trap
209 (soda lime/ Carbosorb) was installed prior to the H_2O trap). The various masses of IAEA-N1
210 used contained between 2.4 and 41.1 μg N. Versteegh et al. (2011) have shown that large masses
211 of $CaCO_3$ do not interfere with low N samples combusted in this manner on a similar

instrumental setup. Percent N was determined on a subset of samples using acetanilide as a standard (10.36% N).

Thirty-three IAEA-N1 standards were analyzed and data were organized into size class bins (Fig. 4). The lower N samples had poorer accuracy (1σ = ~0.5‰ compared to ~0.2‰), but this was not considered problematic considering the large variations expected in the shell $\delta^{15}N$ values. Most of the shell samples produced peaks with an area around 8.5 Vs, which considering the IAEA-N1 data should have an error of less than ± 0.5 ‰ (Fig. 4). Empty tin cups produced very small peaks with an amplitude of ~2 mV or less, i.e. 30 times smaller than our smallest IAEA-N1 peak. We therefore consider ± 0.5 ‰ as a representative uncertainty for all shell $\delta^{15}N$ data, which is conservative considering the reproducibility of 7 homogenized samples noted above (± 0.27 ‰). Shell N concentrations ranged from 0.06 to 0.12 % with an average of 0.09 ± 0.02 % (N=18, collected from two shells). The samples milled adjacent to the original samples in the shell collected in 2000 used to test reproducibility (shell B) had an average difference of 0.2 ± 0.5‰ (n=9) and ranged from 0.0‰ to 1.2‰ different. Although one sample was 1.2‰ different, it was only 0.1‰ off from the preceding sample (see further), thus the samples follow the same pattern as the first set and the new data do not increase the variability in the data. Therefore, the reproducibility is similar to that reported based on the IAEA-N1 data shown in Fig. 4.

3.0 Results

3.1 Depth-transect shells

Carbonate bound organics in shells collected along the depth transect exhibited a wide range of $\delta^{15}N$ values, 1.0‰ to 10.3‰, with a general trend of lower $\delta^{15}N$ values with increasing depth

(Fig 5). The range of values in each shell (intra-shell variability) was highest in the shells from the deepest sites (both = 4.2‰) and lower in shells from shallower sites (1.3‰ to 2.1‰) (Fig. 5). Shell $\delta^{15}N$ values were similar to soft-tissue (adductor muscle) $\delta^{15}N$ values, with the data from the shell edge (representing the most recent time) offering the best correlation with tissue data for shallow water specimens, and the average shell data better correlating for deeper water specimens (Fig 6). Simple linear regression resulted in strong correlations between soft-tissue $\delta^{15}N$ values and both growing shell tip $\delta^{15}N$ values (Fig. 7; R^2=0.992; p<0.0001; n = 6) and average shell $\delta^{15}N$ values (R^2=0.792, p=0.017; n = 6) (Fig. 7). Including data from the three shells collected in 2000 in the regression statistics does not statistically change the goodness of fit (growing shell tip: shell $\delta^{15}N = 0.62 \pm 0.03 *$ tissue $\delta^{15}N + 3.45 \pm 0.27$, $R^2 = 0.98$, $p < 0.0001$; average shell: shell $\delta^{15}N = 0.80 \pm 0.13 *$ tissue $\delta^{15}N + 2.115 \pm 0.98$ (intercept is not significantly different from 0, p = 0.07), $R^2 = 0.847$, p = 0.0004; N = 9 shells for both; standard errors included in regression equations; shell tip slopes (p = 0.51) and intercepts (p = 0.71) were not different, and average shell slopes (p = 0.63) and intercepts were not different (p = 0.74) when the three additional shells were included in the regression).

3.2 High-resolution shell $\delta^{15}N$ profiles

The three shells collected from the Bay of Brest in 2000 and sampled at high resolution show a similar $\delta^{15}N$ pattern, with a high value in late March/ early April, a low around late April/ early May, rising to a high value in late Spring/ early Summer, then decreasing to the end of the growth year (Fig. 8). However, there are large differences between individual shells, up to ~2.5‰ at times, whereas at other times data from different shells converge. The shell $\delta^{15}N$ pattern roughly tracks the digestive gland offset by +3.5‰ pattern (the digestive gland was

emptied prior to analysis and should not contain food; Lorrain et al., 2002). The shell tip $\delta^{15}N$ values versus November adductor muscle tissue $\delta^{15}N$ values plot close to the regression line of the shells collected along the depth transect (Fig. 7).

3.3 Archived shells

The shells from the 1950s, 1965 and 1970s did not show markedly different $\delta^{15}N$ values when compared to shells collected more recently (2000, 2008) in the Bay of Brest (Fig. 9). The 1950s shell has slightly higher $\delta^{15}N$ values compared to the other shells (ANOVA post-hoc Tukey HSD Test $p<0.01$), but overlaps with values from the more recent shells (see Fig. 9).

4.0 Discussion

These data illustrate that shells can be used as archives for nitrogen isotope studies (Fig. 7). The strong correlation between shell and soft-tissue $\delta^{15}N$ values show that shells can be utilized in a similar manner as soft-tissues, which have been extensively utilized to trace pollution, food webs, metabolism, and developing baseline isoscapes (see Fry 1988, 1999; Lorrain et al., 2002; Paulet et al., 2006; Carmichael et al., 2012; Nerot et al., 2012; Vokhshoori and McCarthy, 2014).

4.1 Inter- and intra-shell variability

Pecten maximus shells collected over a large environmental range of $\delta^{15}N$ values strongly correlate with soft-tissues. Individuals that grew in the same area and time can exhibit large offsets in $\delta^{15}N$ profiles, yet exhibit similar intra-annual trends (e.g., up to 2.5‰ between shell B and C in early September; Fig. 8). The differences between the high-resolution shell $\delta^{15}N$ profiles may be caused by several factors. Nitrogen in consumers is typically enriched in ^{15}N by

281 about 3.4‰ (De Niro and Epstein, 1981; Minigawa and Wada, 1984; Vander Zanden and
282 Rasmussen 2001). However, it is well known that N isotope fractionation is a complex process
283 and other factors aside from just trophic enrichment also play a role. Therefore, there is often a
284 large variability in the trophic enrichment factor with standard deviations of more than 1‰ being
285 common (e.g., Post, 2002; Bouillon et al., 2012). Factors such as condition index (animal health),
286 age, food availability, and food quality affect N fractionation (Minagawa and Wada. 1984;
287 Adams and Sterner, 2000; Overman and Parrish, 2001; see Fry, 2006, Caut et al., 2009, and
288 Bouillon et al., 2012, for review). We can rule out food and age as these animals (shells A, B,
289 and C) were growing in the same area and were all the same age class (see Lorrain et al., 2002).
290 The trophic ^{15}N enrichment between a consumer and its food is due to the light isotope, ^{14}N,
291 reacting faster during amino acid deamination thereby enriching ^{15}N in the tissues (Macko et al.,
292 1986). Variations in excretion and nutrient assimilation caused by, for example, condition index
293 or metabolic rate, can therefore result in differences between co-occurring animals (see Fry,
294 2006 for a discussion on N excretion and fractionation), which may explain the differences we
295 see between individuals in Fig. 8.
296
297 Soft-tissues also show variability between individuals (Fig. 6), albeit typically less than seen in
298 these shells (Fig. 8), but soft-tissues integrate more time. Soft-tissues are constantly degrading
299 and are replaced with newly synthesized components in a state of dynamic equilibrium (Bender,
300 1975), thereby updating the isotopic signature of the tissues (e.g., Tieszen, 1978; Tieszen et al.,
301 1983). In general, tissues that are more metabolically active have faster turn-over rates
302 (Thompson and Ballou, 1956; Libby et al., 1964; Paulet et al., 2006). The shells do not have any
303 turn-over and once calcified, the isotope signature is locked in. Sampling of the shells time-

304 averaged about one week of growth (on average; due to shell sampling resolution), whereas the
305 adductor muscle, for example, can integrate several months to years of time due to its slow
306 metabolic turn-over (Lorrain et al. 2002; Paulet et al., 2006; Poulain et al., 2010). Soft-tissue
307 $\delta^{15}N$ values in adductor muscle tissues of this scallop population varied up to 0.8‰ between co-
308 occurring individuals (at the end of March 2000) and up to 1.8‰ in the gonad (at the beginning
309 of May 2000) (Lorrain et al., 2002). *Pecten maximus* adductor muscle tissue has a slower
310 metabolic turn-over than gonad tissue (Paulet et al., 2006), so the adductor muscles are more
311 time-averaged thereby reducing any high-frequency variations. Shells time-average very little
312 time (<1 week), so larger differences between individuals (up to 2.5‰ in our study) are not
313 unexpected. Moreover, the average of high-resolution data (mean of shell A, B and C) shown in
314 Fig. 7 show much less variability between shells (range = 0.4‰), further illustrating the effect of
315 time-averaging on data variability. This can explain why the soft-tissues exhibit much less
316 temporal variability than shells; the soft-tissues average much more time than the shell samples.
317
318 In addition to variability between shells, there are also large seasonal differences in the high-
319 resolution profiles, with up to 3.4‰ variations between April and June for shells B and C (Fig.
320 8). Lorrain et al. (2002) proposed that differences in metabolism and energy allocation have a
321 strong impact on $\delta^{15}N$ values in soft-tissues. For example, large seasonal differences were
322 observed in the digestive gland $\delta^{15}N$ values that were attributed to a shift between utilization of
323 reserves from muscles during the winter to directly from food during phytoplankton events in the
324 spring. Similarly, seasonal variations in adductor muscle $\delta^{15}N$ values were attributed to changes
325 in energy allocation to reproduction. Seasonal changes in energy allocation and metabolism

likely also results in seasonal changes in shell $\delta^{15}N$ values. The analysis of carbonate bound organics therefore opens the possibility to study rapid changes in the metabolism of bivalves.

Despite the observed variations, all three shells analyzed at high-resolution do exhibit similar patterns in $\delta^{15}N$ values (Fig. 8). Moreover, shell $\delta^{15}N$ values are similar to adductor muscle and digestive gland (with a +3.5 offset) $\delta^{15}N$ values, which are smoothed due to slower turn-over rates (Fig. 8). In addition, when the $\delta^{15}N$ values from the growing tips of the shells sampled at high resolution are plotted against the $\delta^{15}N$ values of the adductor muscles at the time of collection, the data lie along the same regression line from the depth transect in Fig. 7. The correlation between soft-tissue and shell $\delta^{15}N$ values suggests that if a sudden large shift in food $\delta^{15}N$ values (i.e., a baseline shift) occurred, for example due to a wastewater pollution event, it may be recorded in high-resolution shell $\delta^{15}N$ values offering the possibility to precisely date such an event. This could prove useful to determine the exact timing and duration of coastal pollution events.

4.2 The shell and soft-tissue $\delta^{15}N$ record of a large nitrogen isotope gradient

The clear decrease seen in both the soft-tissue and shell $\delta^{15}N$ data from the Bay to the edge of the shelf (Fig. 4) is likely caused by less anthropogenic N loading farther from land (see Nerot et al., 2012). However, as noted by Nerot et al. (2012), the $\delta^{15}N$ values of soft-tissues were unexpectedly low in the deeper waters. Considering the 3.5‰ trophic shift, data from deeper scallops suggest a food source with a $\delta^{15}N$ value around 0‰, which is highly unlikely in this region. Nerot et al. (2012) hypothesized that these animals have low metabolic rates due to constant cold-water temperatures coupled with both low food supply and poor food quality (see

also Nerot et al., 2015). Our shell data support this hypothesis, but illustrate that the $\delta^{15}N$ values vary through time, perhaps seasonally. Data from the deepest shell ranged from 1.0 to 5.2‰ (Fig. 5). This variability suggests that there are variations in food supply and quality over time, as well as variations in metabolic activity. As explained above, seasonal variations in shell $\delta^{15}N$ values can be attributed to variations in metabolic activity or energy allocation. The large seasonal differences observed at the deepest sites (as compared to coastal stations) also suggests higher variability in metabolic rates in animals deeper than 150 m water depth, probably due to the sporadic nature of access to food resources.

Metabolic rates and time-averaging can also be used to explain why shells do not plot on the 1:1 line with tissues at the time of collection (Fig. 7). It is possible that during the time of shell collection, metabolic rates in the animals from deeper waters were higher than other times of the year, and therefore there was more N isotope fractionation leading to higher $\delta^{15}N$ values in the shell tip (Fig. 6). The shell tips time-average the recent conditions (~about 1 week) whereas the adductor muscle time-averages several months or longer. This is evident in the deepest shell, where the average shell matches tissue data better than the shell tip (Fig. 6). This illustrates a clear advantage of high-resolution shell sampling; it allows time resolved N isotope data, which provide insight into environmental and biological mechanisms. Nevertheless, it should be noted that there are no *a priori* expectations that the two tissues (muscle and CBOM) should plot on a 1:1 line, as other tissues also do not plot on the 1:1 line, such as muscle and digestive gland tissues (see Fig. 8).

4.3 Archived shells and pollution history

Despite the potential effects of diagenesis on very old shells, dry-stored museum archived shells should remain pristine (discussed in the Introduction; also see Versteegh et al., 2011). In this study, shells collected from the Bay of Brest between the 1950s and 1970s show $\delta^{15}N$ values within the same range of the shells collected in 2000 and 2008, with slightly higher values in the shell collected in the 1950s (Fig. 9). This suggests the Bay would not have undergone significant change over this time period regarding anthropogenic N loading. This corroborates an earlier study that showed there is no indication of any long-term trends in nutrient concentrations between the mid-1970s and early 1990's in the Bay of Brest (see Chauvaud et al., 2000). However, it is known that the sources of N loading to the Bay have changed, with increases in both N from inorganic fertilizer and animal manure (Sebillotte, 1989; Peyraud, et al., 2012), but this is likely rapidly removed due to strong tidal pumping and heavy biological N draw down (Treguer and Queguiner, 1989; Chauvaud et al., 2000). Also, the N isotopic signature of synthetic fertilizer is between +2 and -2‰ because it is synthesized from air via the Haber-Bosch method, whereas pig waste is expected to have higher $\delta^{15}N$ values up to +10 or +20‰ (Heaton, 1986). Therefore, it is possible the N-isotope baseline did not significantly shift because the increase in N loading includes N sources with both low (inorganic fertilizer) and high (pig waste) $\delta^{15}N$ values.

4.4 Potential effects of biomineralization on bulk shell N fractionation

Overall, shell $\delta^{15}N$ values were similar to, or higher than, soft-tissue $\delta^{15}N$ values (Figs. 6 and 8). A survey of literature presenting coupled shell and soft-tissue $\delta^{15}N$ data illustrates that many species with calcite shells also exhibit this pattern, whereas most studies of aragonite shells show the opposite, i.e. lower $\delta^{15}N$ values in the shells than in soft-tissues (Table 1). Considering the

caveat of averaging different amounts of time in soft-tissues (with relatively slow turn-over rates) and shells (with time averaging dependent on sampling resolution and shell growth rate), it can be generalized that carbonate bound organic $\delta^{15}N$ values from calcite shells match soft-tissue $\delta^{15}N$ values, whereas carbonate bound organic $\delta^{15}N$ values from aragonite shells are closer to $\delta^{15}N$ values of particulate organic matter (i.e., the bivalve's food). It has been shown that calcite prisms and aragonitic nacre are built using very different proteins (Marie et al., 2012); therefore it can be assumed that calcite shells and aragonite shells also use a different set of proteins. It is also well known that different proteins or amino acids (the building blocks of proteins) have largely different $\delta^{15}N$ values (McClelland and Montoya, 2002; Vokhshoori and McCarthy, 2014). Therefore, we hypothesize that the differences observed between calcite and aragonite soft-tissue / shell $\delta^{15}N$ values ($\Delta_{tissue\text{-}shell}$) could be the result of different amino acid groups present in the different mineral types, and that these different amino acids are somewhat common in shells with the same $CaCO_3$ polymorph.

4.5 Suggestions for future research: CSIA

Future work on nitrogen isotopes in carbonate bound organics should investigate the $\delta^{15}N$ values of specific amino acids for several reasons. First, this could help develop the biomineralization hypothesis we propose above in Section 4.4. Second, compound specific isotope analysis (CSIA) could also pinpoint amino acids that specifically record baseline $\delta^{15}N$ values (cf., Vokhshoori and McCarthy, 2014; McMahon et al., 2015). Finally, CSIA could potentially reveal amino acids that are more resistant to diagenesis. Studies have shown that on time scales of 10,000 years to millions of years, carbonate bound organic material is subject to diagenesis depending on burial history, shell thickness, and mineralogy (Robbins and Ostrom, 1995; Risk et al., 1996).

However, other studies have shown some amino acids to be stable on century time scales in porous coral skeletons (Goodfriend et al., 1992; Ingalls et al., 2003), and even more than 100,000 year time scales in well-preserved mollusk shells (Engel et al., 1994).

5.0 Conclusions

In conclusion, we show that simple combustion of shell material in an EA permits very low %N samples to be easily analyzed with minimal processing, allowing increased temporal resolution up to approximately one week. Our high-resolution results suggest that metabolism and/or energy allocation can affect shell $\delta^{15}N$ values (as it does soft-tissue $\delta^{15}N$ values), but that seasonal and spatial variation shows good correlation with soft-tissue $\delta^{15}N$ values. These carbonate bound organic $\delta^{15}N$ values would then be particularly useful to track both modern and past isotope spatial gradients (isoscapes of $\delta^{15}N$ values) across various systems, monitoring nitrogen regime shifts due to pollution or natural N cycle processes. In addition, other natural variations in particulate $\delta^{15}N$ values caused, for example, by upwelling, could also be preserved in shell organics, potentially serving as an upwelling / El Niño Southern Oscillation proxy. Overall, carbonate-bound organic matter is a good archive of soft-tissue $\delta^{15}N$ values and offers the possibility to examine $\delta^{15}N$ shifts at high-resolution.

Acknowledgements

We thank Jean-Marie Munaron for milling all shells for this study, David Dettman for useful discussions on combusting shells for $\delta^{15}N$ analysis, Ruth Carmichael for discussions on CBOM $\delta^{15}N$ analysis methods, and shells collectors (YM Paulet, J. Grall, and M. Glemarec). We also thank Alan Wanamaker, Anouk Verheyden, three anonymous reviewers, and Ethan Grossman

for constructive comments on earlier versions of this manuscript, and Roger Hoerl who helped with statistical tests. This study was funded by the French GIS Europole Mer, EC2CO PNEC ISOBENT, EC2CO PNEC, CYTRIX IBANOE, the Fund for Scientific Research-Flanders (FWO, project G.0D87.14N), and the Special Research Fund of the KU Leuven (Belgium). We also thank the US National Science Foundation for funding Union College's isotope ratio mass spectrometer and peripherals (NSF-MRI #1229258) on which some methods were developed and/or tested.

References

Adams T.S., Sterner R.W., 2000. The effect of dietary nitrogen content on trophic level ^{15}N enrichment. *Limnol. Oceanog*. **45**, 601–607.

Bender D.A., 1975. *Amino acid metabolism*. New York: John Wiley & Sons 1975.

Bentis C. J., Kaufman L., Golubic S., 2000. Endolithic fungi in reef-building corals (Order: Scleractinia) are common, cosmopolitan, and potentially pathogenic. *Biol. Bull.* **198(2)**, 254-260.

Bouillon S., Connolly R.M., Gillikin D.P., 2012. Use of stable isotopes to understand food webs and ecosystem functioning in estuaries. In: Heip C, Philippart K, & Middelburg JJ (eds) *Ecosystem processes in estuaries and coasts*. Volume **7** of Wolanski & McLusky (eds) Treatise on Estuarine and Coastal Science. Elsevier Pages 143-173. doi: 10.1016/B978-0-12-374711-2.00711-7

Butler P.G., Wanamaker A.D., Jr., Scourse J.D., Richardson C.A., Reynolds D.R., 2013. Variability of marine climate on the North Icelandic Shelf in a 1357-year proxy archive based on growth increments in the bivalve *Arctica islandica*. *Palaeogeogr. Palaeoclimatol. Palaeoecol*., **373**, 141-151, doi:10.1016/j.palaeo.2012.01.016.

Cabana G., Rasmussen J.B., 1996. Comparison of aquatic food chains using nitrogen isotopes. *Proc. Natl. Acad. Sci. U.S.A.* **93(20)**, 10844-10847.

Carabel S., Verısimo P., Freire J., 2009. Effects of preservatives on stable isotope analyses of four marine species. *Estuar. Coast. Shelf. Sci*. **82**, 348-350.

Carmichael R.H., Hattenrath T., Valiela I., Michener R.H., 2008. Nitrogen stable isotopes in the shell of *Mercenaria mercenaria* trace wastewater inputs from watersheds to estuarine ecosystems. *Aquatic Biol*. **4**, 99-111.

Carmichael R.H., Shriver A.C., Valiela I. (2012). Bivalve response to estuarine eutrophication: the balance between enhanced food supply and habitat alterations. *J. Shellfish Res*. **31(1)**, 1-11.

Caut S., Angulo E., Courchamp F., 2009. Variation in discrimination factors (Δ15N and Δ13C): the effect of diet isotopic values and applications for diet reconstruction. *J. Applied Ecology* **46(2)**, 443-453.

Chauvaud L., Jean F., Ragueneau O., Thouzeau G., 2000. Long-term variation of the Bay of Brest ecosystem: benthic-pelagic coupling revisited. *Mar. Ecol. Prog. Ser.* **200**, 35-48

Cole J. J., Carpenter S. R., Kitchell J., Pace M. L., Solomon C. T. Weidel, B., 2011. Strong evidence for terrestrial support of zooplankton in small lakes based on stable isotopes of carbon, nitrogen, and hydrogen. *Proc. Natl. Acad. Sci. U.S.A.* **108(5)**, 1975-1980.

Costanzo S.D., Udy J., Longstaff B., Jones A., 2005. Using nitrogen stable isotope ratios ($\delta^{15}N$) of macroalgae to determine the effectiveness of sewage upgrades: changes in the extent of sewage plumes over four years in Moreton Bay, Australia. *Mar. Poll. Bull*. **51(1)**, 212-217.

Delong M.D., Thorp J.H., 2009. Mollusc shell periostracum as an alternative to tissue in isotopic studies. *Limnol. Oceanog.: Methods* **7(6)**, 436-441.

DeNiro M.J., Epstein S., 1981. Influence of diet on the distribution of nitrogen isotopes in animals. *Geochim. Cosmochim. Acta* **45**, 341-351.

Dreier A., Stannek L., Blumenberg M., Taviani M., Sigovini M., Wrede C., Thiel V., Hoppert M., 2012. The fingerprint of chemosymbiosis: origin and preservation of isotopic biosignatures in the nonseep bivalve *Loripes lacteus* compared with *Venerupis aurea*. *FEMS Microbiology Ecology* **81(2)**, 480-493.

Engel M.H., Goodfriend G.A., Qian Y., Macko S.A., 1994. Indigeneity of organic matter in fossils: a test using stable isotope analysis of amino acid enantiomers in Quaternary mollusk shells. *Proc. Natl. Acad. Sci. U.S.A.* **91(22)**, 10475-10478.

Erler D.V., Wang X.T., Sigman D.M., Scheffers S.R., Martínez-García A., Haug G.H., 2016. Nitrogen isotopic composition of organic matter from a 168 year-old coral skeleton:

Implications for coastal nutrient cycling in the Great Barrier Reef Lagoon. Earth Planet. Sci. Lett. **434**, 161-170.

Fry B., 1988. Food web structure on Georges Bank from stable C, N, and S isotopic compositions. *Limnol. Oceanog*. **33**, 1182-1190.

Fry B., 1999. Using stable isotopes to monitor watershed influences on aquatic trophodynamics. *Can. J. Fish. Aquat. Sci*. **56**, 2167e2171.

Fry, B., 2006. Stable Isotope Ecology. Springer, New York.

Gillikin D.P., Lorrain A., Paulet Y.-M., André L., Dehairs F., 2008. Synchronous barium peaks in high-resolution profiles of calcite and aragonite marine bivalve shells. *Geo-Mar. Lett*. **28**: 351-358.

Gillikin D.P., Lorrain A., Bouillon S., Versteegh E.A., Yambélé A., Graniero L., Charles D., Jolivet A., 2012. Nitrogen isotopes in the organic matrix of bivalve shells: a recorder of anthropogenic nitrogen pollution. *2012 Ocean Sciences Meeting, Salt Lake City UT*.

Goodfriend G.A., Hare P.E., Dreffel E.R.M., 1992. Aspartic acid racemization and protein diagenesis in corals over the last 350 years. *Geochim. Cosmochim. Acta* **56**, 3847–3850.

Goodwin D.H., Schöne B.R., Dettman D.L., 2003. Resolution and fidelity of oxygen isotopes as paleotemperature proxies in bivalve mollusk shells: models and observations. *Palaios* **18 (2)**, 110-125.

Graniero L.E., Grossman E.L., O'Dea A., 2016. Stable isotopes in bivalves as indicators of nutrient source in coastal waters in the Bocas del Toro Archipelago, Panama. PeerJ 4:e2278; DOI 10.7717/peerj.2278

Grønkjær P., Pedersen J.B., Ankjærø T.T., Kjeldsen H., Heinemeier J., Steingrund P., Nielsen J.M., Christensen J.T., 2013. Stable N and C isotopes in the organic matrix of fish otoliths: validation of a new approach for studying spatial and temporal changes in the trophic structure of aquatic ecosystems. *Can. J.Fish. Aquat. Sci*. **70(2)**, 143-146.

Heaton T.H.E. (1986). Isotopic studies of nitrogen pollution in the hydrosphere and atmosphere: a review. *Chem. Geo*. **59**, 87-102.

Ingalls A.E., Lee C., Druffel E.R., 2003. Preservation of organic matter in mound-forming coral skeletons. *Geochim. Cosmochim. Acta* **67(15)**, 2827-2841.

Jacob U., Mintenbeck K., Brey T., Knust R., Beyer K., 2005. Stable isotope food web studies: a case for standardized sample treatment. *Mar. Ecol. Prog. Ser.* **287**, 251-253.

Jennings S., Warr K.J., 2003. Environmental correlates of large-scale spatial variation in the $\delta^{15}N$ of marine animals. *Mar. Biol*. **142**, 1131–1140. doi:10.1007/s00227-003-1020-0.

Kovacs C.J., Daskin J.H., Patterson H., Carmichael R.H., 2010. *Crassostrea virginica* shells record local variation in wastewater inputs to a coastal estuary. *Aquat. Biol*. **9**: 77–84 doi: 10.3354/ab00228

LeBlanc C., 1989. Terrestrial input to estuarine bivalves as measured by multiple stable isotopes tracers. PhD thesis, McMaster, Montreal, Canada.

Libby W.F., Berger R., Mead J., Alexander G., Ross J., 1964. Replacement rates for human tissue from atmospheric radiocarbon. *Science* **146** : 1170-1172

Lorrain A., Paulet Y.M., Chauvaud L., Dunbar R., Mucciarone D., Fontugne M., 2004. $\delta^{13}C$ variation in scallop shells: increasing metabolic carbon contribution with body size? *Geochim. Cosmochim. Acta* **68(17)**, 3509-3519.

Lorrain A., Paulet Y.M., Chauvaud L., Savoye N., Donval A., Saout C., 2002. Differential $\delta^{13}C$ and $\delta^{15}N$ signatures among scallop tissues: implications for ecology and physiology. *J. Exp. Mar. Biol. Ecol.* **275(1)**, 47-61.

Macko S.A., Fogel Estep M.L., Engel M.H., Hare P.E., 1986. Kinetic fractionation of stable nitrogen isotopes during amino acid transamination. *Geochim. Cosmochim. Acta* **50**, 2143–2146.

Marie B., Joubert C., Tayalé A., Zanella-Cléon I., Belliard C., Piquemal D., Cochennec-Laureau N., Marin F., Gueguen Y., Montagnani C., 2012. Different secretory repertoires control the biomineralization processes of prism and nacre deposition of the pearl oyster shell. *Proc. Natl. Acad. Sci. U.S.A.* **109(51)**, 20986-20991

Marin F., Luquet G., Marie B., Medakovic, D., 2007. Molluscan shell proteins: primary structure, origin, and evolution. *Current Topics In Developmental Biology **80***, 209-276.

Marin F., Luquet G., 2004. Molluscan shell proteins. *Comptes Rendus Palevol, Biomineralisation : Diversite et Unite* **3**, 469–492. doi:10.1016/j.crpv.2004.07.009

Marion G.S., Dunbar R.B., Mucciarone D.A., Kremer J.N., Lansing J.S., Arthawiguna A., 2005. Coral skeletal $\delta^{15}N$ reveals isotopic traces of an agricultural revolution. *Mar. Poll. Bull.* **50(9)**, 931-944.

Marwick T.R., Tamooh F., Ogwoka B., Teodoru C., Borges A.V., Darchambeau F., Bouillon S., 2014. Dynamic seasonal nitrogen cycling in response to anthropogenic N loading in a

561 tropical catchment, Athi–Galana–Sabaki River, Kenya. *Biogeosciences* **11**, 443-460,
562 doi:10.5194/bg-11-443-2014.
563 Mateo M., Serrano O., Serrano L., Michener R., 2008. Effects of sample preparation on stable
564 isotope ratios of carbon and nitrogen in marine invertebrates: implications for food web
565 studies using stable isotopes. *Oecologia* **157**, 105-115.
566 McClelland J.W., Montoya J.P., 2002: Trophic relationships and the nitrogen isotopic
567 composition of amino acids in plankton. *Ecology* **83**, 2173-2180.
568 McMahon K.W., Hamady L.L., Thorrold S.R., 2013. A review of ecogeochemistry approaches
569 to estimating movements of marine animals. *Limnol. Oceangr*. **58**, 697–714
570 doi:10.4319/lo.2013.58.2.0697
571 McMahon K.W., Thorrold S.R., Elsdon T.S., McCarthy M.D., 2015. Trophic discrimination of
572 nitrogen stable isotopes in amino acids varies with diet quality in a marine fish. *Limnol.*
573 *Oceanogr.* **60**, 1076-1087.
574 Minagawa M., Wada E., 1984. Stepwise enrichment of ^{15}N along food chains: further evidence
575 and the relation between δ^{15}N and animal age. *Geochim. Cosmochim. Acta* **48(5)**, 1135-
576 1140.
577 Mollier-Vogel E., Ryabenko E., Martinez P., Wallace D., Altabet M. A., Schneider R., 2012.
578 Nitrogen isotope gradients off Peru and Ecuador related to upwelling, productivity, nutrient
579 uptake and oxygen deficiency. *Deep-Sea Res. Pt I* **70**, 14-25.
580 Nerot C., Lorrain A., Grall J., Gillikin D.P., Munaron J.-M., Le Bris H., Paulet Y.-M., 2012.
581 Stable isotope variations in benthic filter feeders across a large depth gradient on the
582 continental shelf. *Est. Coast. Shelf Sci*. **96**, 228-235. doi:10.1016/j.ecss.2011.11.004.
583 Nerot C., Meziane T., Schaal G., Grall J., Lorrain A., Paulet Y. M., Kraffe E., 2015. Spatial
584 changes in fatty acids signatures of the great scallop *Pecten maximus* across the Bay of
585 Biscay continental shelf. *Cont. Shelf Res*. **109**, 1-9.
586 Ng J.S.S., Wai T.-C., Williams G.A., 2007. The effects of acidification on the stable isotope
587 signatures of marine algae and molluscs. *Mar. Chem*. **103**, 97-102.
588 O'Donnell T.H., Macko S.A., Chou J., Davis-Hartten K.L., Wehmiller J.F., 2003. Analysis of
589 δ^{13}C, δ^{15}N, and δ^{34}S in organic matter from the biominerals of modern and fossil
590 *Mercenaria* spp. *Org. Geochem*. **34**, 165-183.
591 O'Donnell T., Macko S.A., Wehmiller J., 2007. Stable carbon isotope composition of amino

592 acids in modern and fossil *Mercenaria*. *Org. Geochem*. **38**, 485– 498.
593 Overman N.C., Parrish D.L., 2001. Stable isotope composition of walleye: ^{15}N accumulation
594 with age and area-specific differences in $\delta^{13}C$. *Can. J. Fish. Aquat. Sci*. **58**, 1253–1260.
595 Paulet Y.M., Lorrain A., Richard J., Pouvreau S., 2006. Experimental shift in diet $\delta^{13}C$: A
596 potential tool for ecophysiological studies in marine bivalves. *Org. Geochem*. **37(10)**,
597 1359-1370.
598 Peyraud J.-L., Cellier P., Donnars C., Réchauchère O., (editors), 2012. *Les flux d'azote liés aux*
599 *élevages, réduire les pertes, rétablir les équilibres. Expertise scientifique collective,*
600 *synthèse du rapport*, INRA (France), 68 p.
601 Post D.M., 2002. Using stable isotopes to estimate trophic position: models, methods, and
602 assumptions. *Ecology* **83**, 703-718.
603 Poulain C., Lorrain A., Mas R., Gillikin D.P., Dehairs F., Robert R., Paulet Y.-M., 2010.
604 Experimental shift of diet and DIC stable carbon isotopes: Influence on shell $\delta^{13}C$ values in
605 the Manila clam *Ruditapes philippinarum*. *Chem. Geol*. **272(1)**, 75-82.
606 Ren H., Sigman D.M., Chen M.T., Kao S.J., 2012a. Elevated foraminifera- bound nitrogen
607 isotopic composition during the last ice age in the South China Sea and its global and
608 regional implications. *Global Biogeochem. Cy.* **26**, GB1031, doi:10.1029/2010GB004020.
609 Ren H., Sigman D.M., Thunell R.C., Prokopenko M.G., 2012b. Nitrogen isotopic composition of
610 planktonic foraminifera from the modern ocean and recent sediments. *Limnol. Oceanogr.*
611 *57(4)*, 1011-1024.
612 Ren H., Sigman D.M., Meckler A.N., Plessen B., Robinson R.S., Rosenthal Y., Haug G.H.,
613 2009. Foraminiferal isotope evidence of reduced nitrogen fixation in the ice age Atlantic
614 Ocean. *Science* **323(5911)**, 244-248.
615 Risk M.J., Sayer B.G., Tevesz M.J., Karr C.D., 1996. Comparison of the organic matrix of fossil
616 and recent bivalve shells. *Lethaia* **29(2)**, 197-202.
617 Robbins L.L., Ostrom P.H., 1995. Molecular isotopic and biochemical evidence of the origin and
618 diagenesis of shell organic material. *Geology* **23(4)**, 345-348.
619 Robinson R.S., Kienast M., Luiza Albuquerque A., Altabet M., Contreras S., De Pol Holz R.,
620 Dubois N., Francois R., Galbraith E., Hsu T.C. Ivanochko T., Jaccard S., Kao S.J.,
621 McCarthy M., Möbius J., Pedersen T., Quan T.M., Ryabenko E., Schmittner A., Schneider
622 R., Schneider-Mor A., Shigemitsu M., Sinclair D., Somes C., Studer A., Thunell R., Yang

623 J. Y., 2012. A review of nitrogen isotopic alteration in marine sediments.
624 *Paleoceanography* **27** PA4203, doi:10.1029/2012PA002321.
625 Rowell K., Dettman D.L., Dietz R., 2010. Nitrogen isotopes in otoliths reconstruct ancient
626 trophic position. *Environ. Biol. Fish.* **89(3-4)**, 415-425.
627 Schlacher T.A., Mondon J.A., Connolly R.M., 2007. Estuarine fish health assessment: evidence
628 of wastewater impacts based on nitrogen isotopes and histopathology. *Mar. Poll. Bull*. **54**,
629 1762–1776.
630 Sebillotte M., 1989. *Fertilité et systèmes de productions*. Publication INRA. 370pp.
631 Serrano O., Serrano L., Mateo M. A., Colombini I., Chelazzi L., Gagnarli E., Fallaci M., 2008.
632 Acid washing effect on elemental and isotopic composition of whole beach arthropods:
633 implications for food web studies using stable isotopes. *Acta Oecol*. **34(1)**, 89-96.
634 Susic M., Boto, K., Isdale P., 1991. Fluorescent humic acid bands in coral skeletons originate
635 from terrestrial runoff. *Mar. Chem.* **33(1)**, 91-104.
636 Thompson R.C., Ballou J.E., 1956. Studies of metabolic turnover with tritium as a tracer. V. The
637 predominantly non-dynamic state of body constituents in the rat. *J Biol Chem* **223**, 795-
638 809.
639 Tieszen L.L., 1978. Carbon isotope fractionation in biological material. *Nature* **276**, 97-98.
640 Tieszen L.L., Boutton T.W., Tesdahl K.G., Slade N.A., 1983. Fractionation and turn-over of
641 stable carbon isotopes in animal tissues: implications for $\delta^{13}C$ analysis of diet. *Oecologia*
642 **57**, 32–37.
643 Treguer P., Queguiner B., 1989. Conservative and non conservative mixing of dissolved and
644 particulate nitrogen compounds, with respects to seasonal variability, in a West European
645 macrotidal estuary. *Oceanol. Acta* **12**, 371-380
646 Vander Zanden M., Rasmussen J. B., 2001. Variation in $\delta^{15}N$ and $\delta^{13}C$ trophic fractionation:
647 implications for aquatic food web studies. *Limnol. Oceanogr*. **46(8)**, 2061-2066.
648 Vandermyde J.M., G.W. Whitledge 2008. Otolith $\delta^{15}N$ distinguishes fish from forested and
649 agricultural streams in southern Illinois. *J. Freshwater Ecol*. **23**, 333-336.
650 Versteegh E.A.A., Gillikin D.P., Dehairs F., 2011. Analysis of $\delta^{15}N$ values in mollusk shell
651 organic matrix by EA-IRMS without acidification: an evaluation and effects of long-term
652 preservation. *Rapid Comm. Mass Spectr*. **25**, 675-680. doi: 10.1002/rcm.4905

Vokhshoori N.L., McCarthy M.D., 2014. Compound-specific $\delta^{15}N$ amino acid measurements in littoral mussels in the California upwelling ecosystem: A new approach to generating baseline $\delta^{15}N$ isoscapes for coastal ecosystems. *PLoS ONE* **9(6)**: e98087. doi:10.1371/journal.pone.0098087

Wang X.T., Sigman D.M., Cohen A.L., Sinclair D.J., Sherrell R.M., Weigand M.A., Erler D.V., Ren H., 2015. Isotopic composition of skeleton-bound organic nitrogen in reef-building symbiotic corals: a new method and proxy evaluation at Bermuda. *Geochim. Cosmochim. Acta* **148**, 179-190.

Watanabe S., Kodama M., Fukuda M., 2009. Nitrogen stable isotope ratio in the Manila Clam, *Ruditapes philippinarum*, reflects eutrophication levels in tidal flats. *Mar. Pollut. Bull*. **58**, 1447-1453.

Williams B., Grottoli A.G. (2010). Stable nitrogen and carbon isotope ($\delta^{15}N$ and $\delta^{13}C$) variability in shallow tropical Pacific soft coral and black coral taxa and implications for paleoceanographic reconstructions. *Geochim. Cosmochim. Acta* **74(18)**, 5280-5288.

Yamazaki A., Watanabe T., Tsunogai U., 2011a. $\delta^{15}N$ in reef coral skeletons as a proxy of tropical nutrient dynamics. *Geophys. Res. Lett*. **38**, L19605, doi:10.1029/2011GL049053.

Yamazaki A., Watanabe T., Ogawa N., Ohkouchi N., Shirai K., Toratani M., Uematsu M., 2011b. Seasonal variations in the nitrogen isotope composition of Okinotori coral in the tropical Western Pacific: A new proxy for marine nitrate dynamics. *J. Geophys. Res*. **116**, G04005, doi:10.1029/2011JG001697.

Yamazaki A., Watanabe T., Takahata N., Sano Y., Tsunogai U., 2013. Nitrogen isotopes in intra-crystal coralline aragonites. *Chem. Geol*. **351**, 276–280, doi:10.1016/j.chemgeo.2013.05.024.

682

683 **Table 1.** Differences between soft-tissue and carbonate bound organics ($\Delta_{tissue\text{-}shell}$) and
684 shell mineralogy (C = calcite, A = aragonite) for 11 bivalve species.
685

Species	Mineralogy	$\Delta_{tissue\text{-}shell}$ (‰)	Source
Pecten maximus	C	-1.3	This study
Mytilus edulis	C	-2.3	Versteegh et al. (2011)
Crassostrea virginica	C	-0.2	Kovacs et al. (2010)
Mytilus edulis	C+A?	-0.1*	LeBlanc (1989)
Pinctada imbricata	C+A?	~0.0*	Graniero et al. (2016)
Isognomon alatus	C+A?	~0.0*	Graniero et al. (2016)
Brachidontes exustus	C+A?	~0.0*	Graniero et al. (2016)
Arctica islandica	A	+2.7	LeBlanc (1989)
Ruditapes philippinarum	A	+1.1	Wananabe et al. (2009)
Mercenaria mercenaria	A	+2.4	Carmichael et al. (2008)
Mercenaria mercenaria	A	+1.0	O'Donnell et al. (2003)
Chambardia wissmanni	A	+3.0	Gillikin et al. (2012)
Venerupis aurea	A	+6.2	Dreier et al. (2012)

686 To be consistent, adductor muscle values were used when $\delta^{15}N$ values were available from
687 multiple tissues. Only non-transplanted specimens were used from Kovacs et al. (2010)
688 because the muscle tissues of transplanted animals may have not yet equilibrated with the
689 new environment. All species are estuarine or marine except for *C. wissmanni*, which is an
690 African tropical freshwater mussel. *These studies may have mixed aragonite and calcite
691 layers, but this is not certain.

Figure legends:

Figure 1. Map of study area in northern Bay of Biscay with shell collection sites (black circles) and collection depth. Bathymetry contours are in meters.

Figure 2. Schematic of shell sampling. Fine grey lines represent daily striae and dark lines are winter lines indicating growth cessation. Short thick lines represent areas milled for CBOM samples. A) lower resolution sampling of older shells along depth transect. B) High-resolution sampling of younger shells from the Bay of Brest (collected in 2000).

Figure 3. Comparison of $\delta^{15}N$ data measured on bleached and unbleached halves of the same growth striae from the same *Pecten maximus* valve. Growth and time is from sample 1 to 4 (left to right). Error bars represent ±0.5‰ (see text).

Figure 4. Average and standard deviations (1σ) for various sized IAEA-N1 standards. Values are binned into ranges of nitrogen mass (x-axis). Standard deviations (1σ) are also listed below each data point. The average and standard deviation for N1 reported by the IAEA is also shown for comparison (shown as IAEA on x-axis). Number of standards analyzed from low to high N is 10, 10, 9, and 4. Peak amplitude for mass 28 (in mV) ranged from 60 to 100, 125 to 220, 300 to 425, 800 to 1200, whereas peak area (in Vs) ranged from 2 to 5, 5 to 10, 10 to 20, and > 20 from low N to high N.

Figure 5. Shell $\delta^{15}N$ values for samples milled from shells collected at different depths (one shell per depth). The white symbols represent the sample taken from the tip of the shell, so the most recent shell material, and black symbols represent time earlier in the growth year. Error bar shows ±0.5‰ (see text).

Figure 6. Average and shell tip $\delta^{15}N$ values plotted against soft-tissue $\delta^{15}N$ values from *P. maximus* collected along the same transect. Soft-tissue $\delta^{15}N$ values from Nerot et al. (2012).

715 Figure 7. Simple linear regression of average (grey) and shell tip (black) $\delta^{15}N$ values plotted
716 against soft-tissue $\delta^{15}N$ values (standard errors included). Also shown are the averages of the
717 shells sampled at high resolution (small black symbols). The grey dashed line is the 1:1 line.
718 Figure 8. High-resolution shell $\delta^{15}N$ values plotted against growth date (3 shells). Also shown
719 are $\delta^{15}N$ values of adductor muscle and digestive gland. For easier comparison, 3.5‰ was added
720 to the digestive gland data (shaded circles). Thin grey line represents daily shell growth rate
721 based on growth striae. Soft-tissue and shell growth data from Lorrain et al. (2002). Open
722 symbols of Shell B are additional (replicate) samples analyzed on a different day (see text).
723 Figure 9. Shell $\delta^{15}N$ values from museum archived shells. Black symbols represent data over the
724 annual growth of one specimen; white circle is the average of the shell. 21st century shell data are
725 from the shells sampled at high-resolution in Fig. 7 and the shell from the Bay (40m) in Fig. 4
726 (totaling 4 shells).

Figure 1

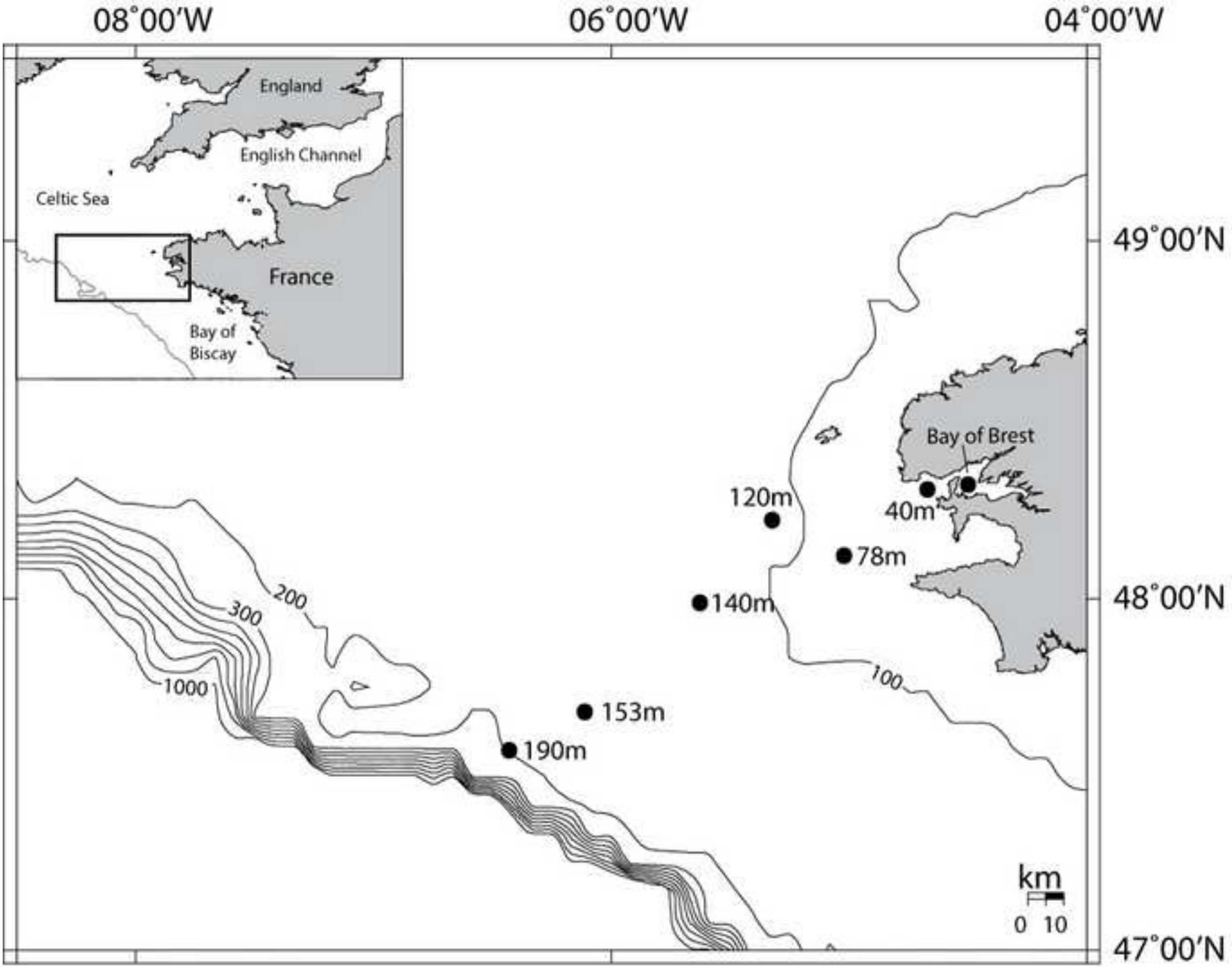
08°00'W
06°00'W
04°00'W
49°00'N
48°00'N
47°00'N
England
English Channel
Celtic Sea
France
Bay of
Biscay
Bay of Brest
120m
40m
78m
140m
153m
190m
200
300
1000
100
km
0 10

Figure 2

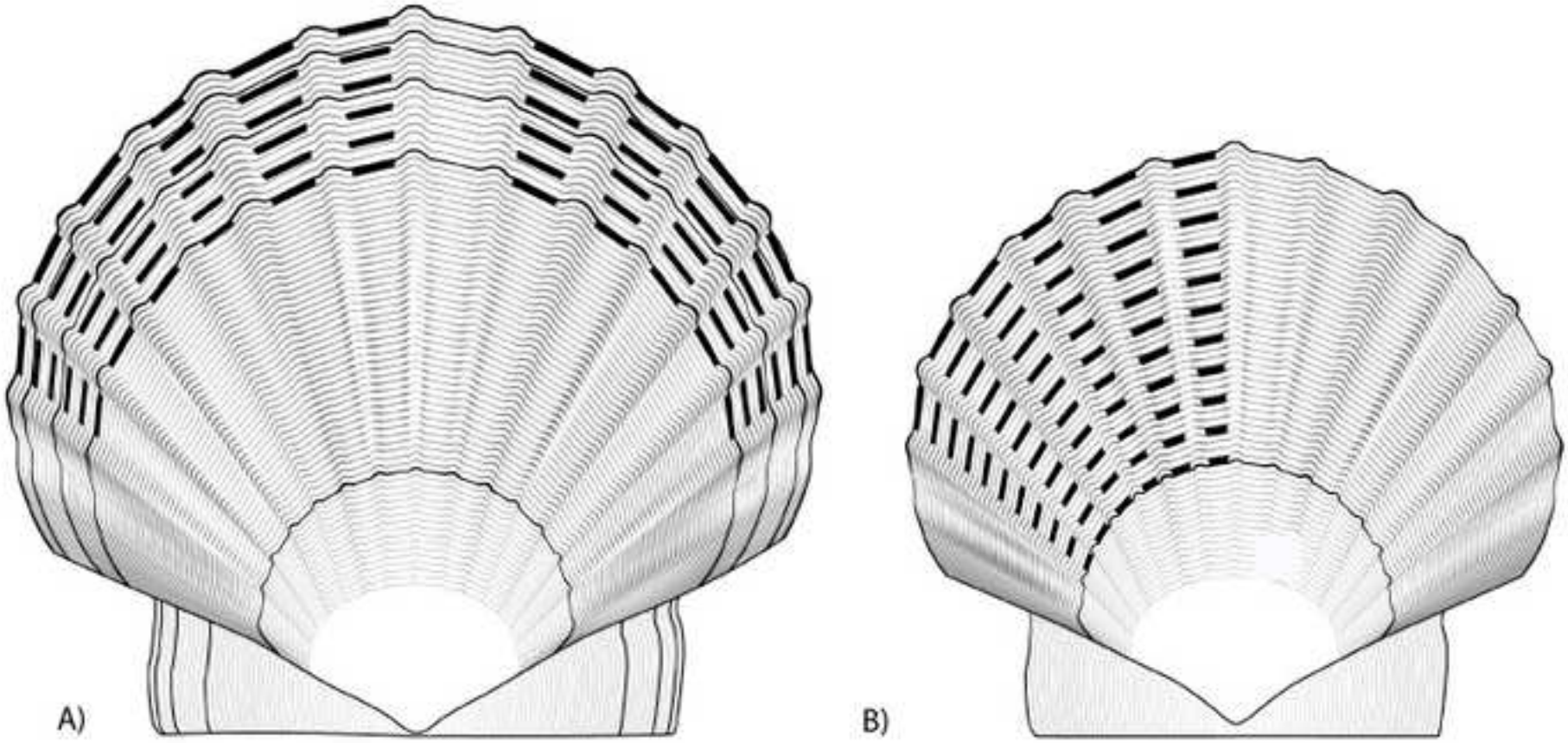

Figure 3

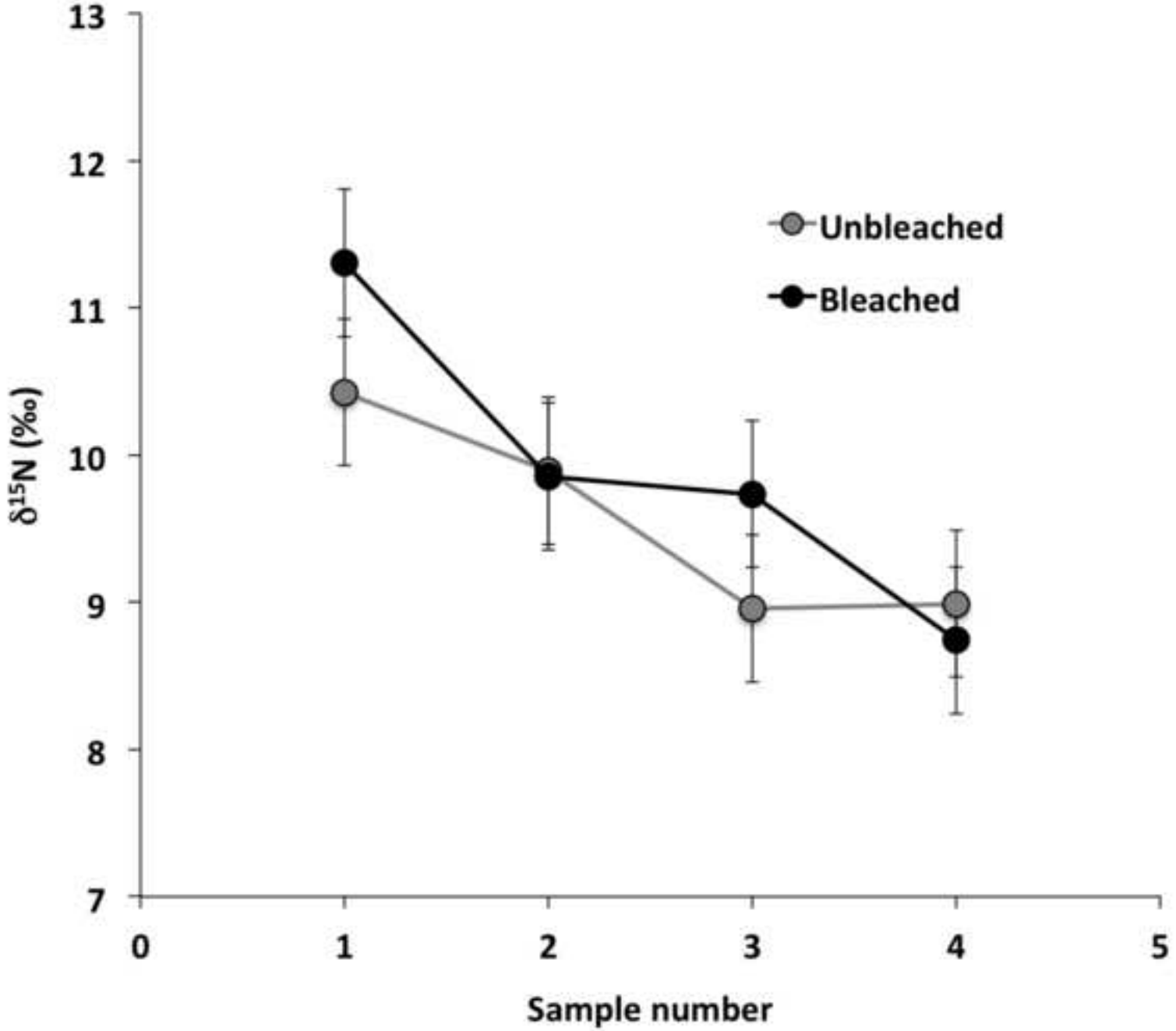
13
12
11
10
9
8
7
δ15N (‰)
0
1
2
3
4
5
Sample number
Unbleached
Bleached

Figure 4

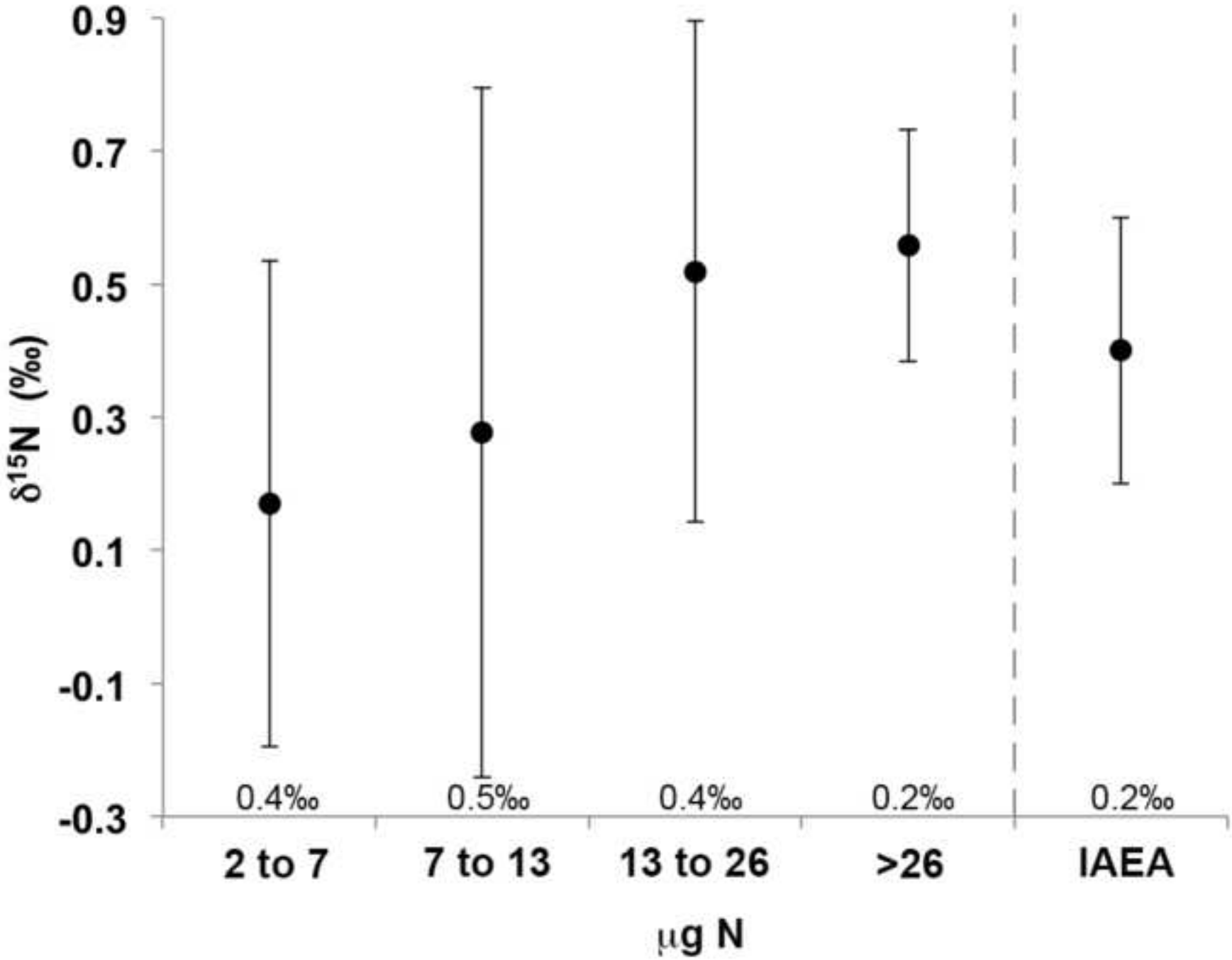
0.9
0.7
0.5
0.3
0.1
-0.1
-0.3
δ15N (‰)
0.4‰
0.5‰
0.4‰
0.2‰
0.2‰
2 to 7
7 to 13
13 to 26
>26
IAEA
μg N

Figure 5

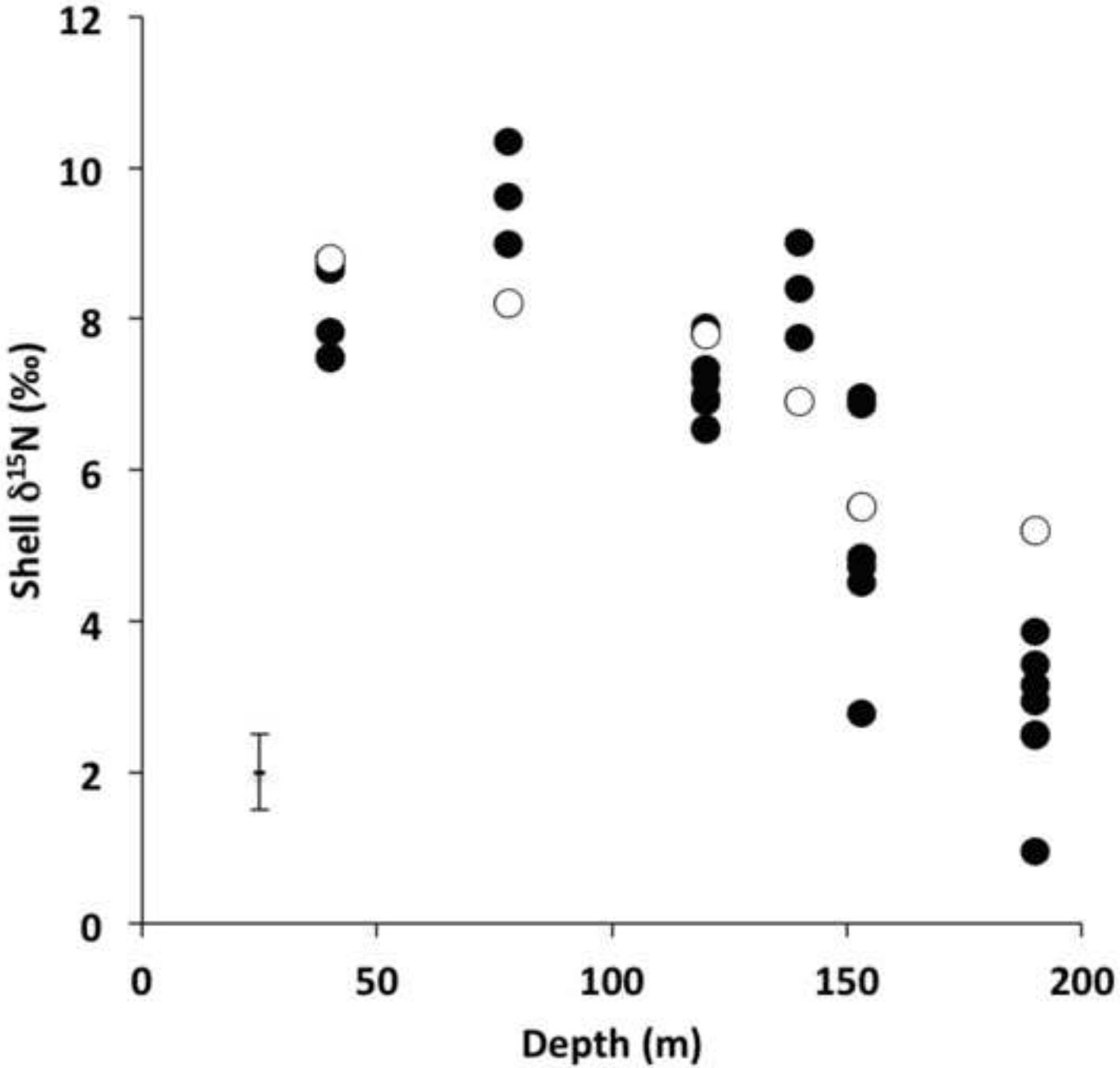

Figure 6

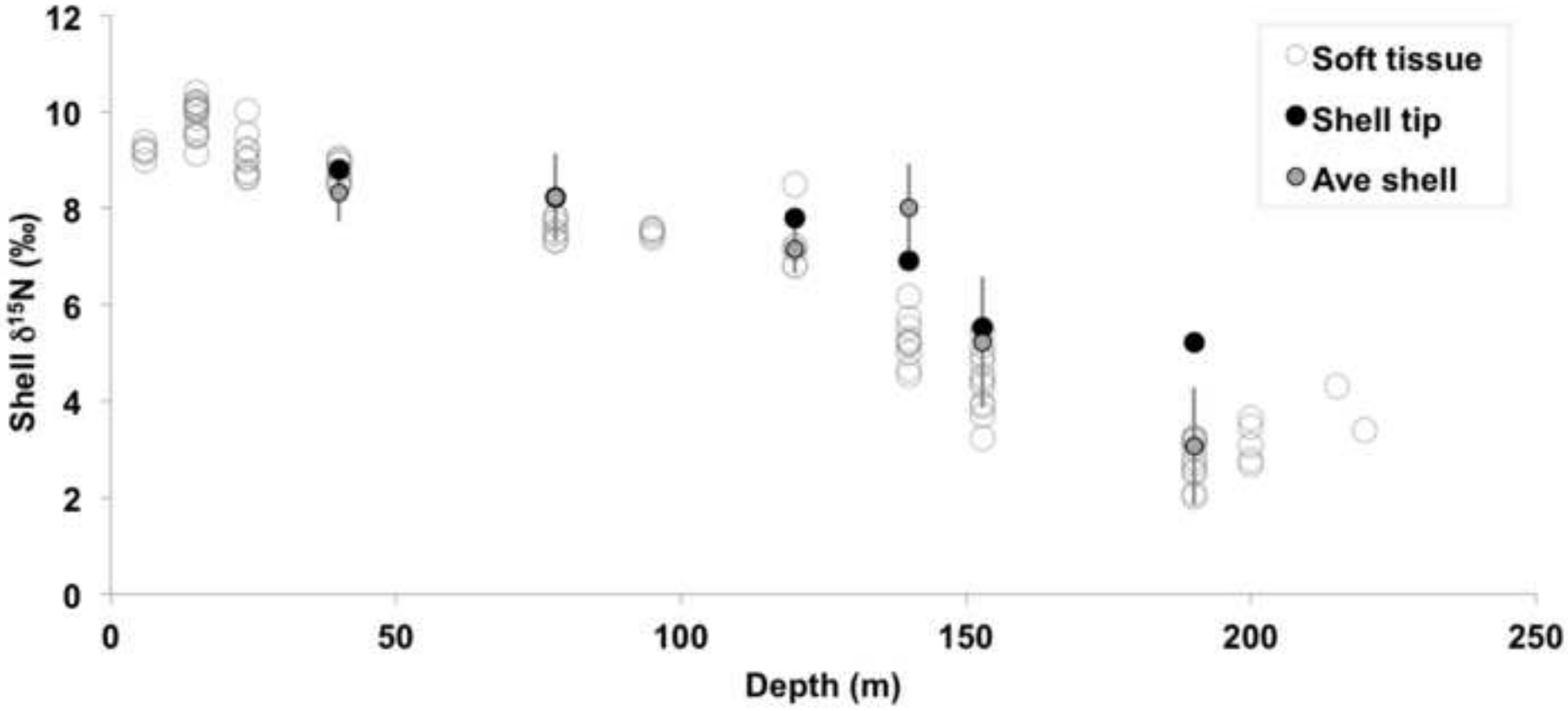
Soft tissue
Shell tip
Ave shell
Shell δ15N (‰)
Depth (m)
0
2
4
6
8
10
12
0
50
100
150
200
250

Figure 7

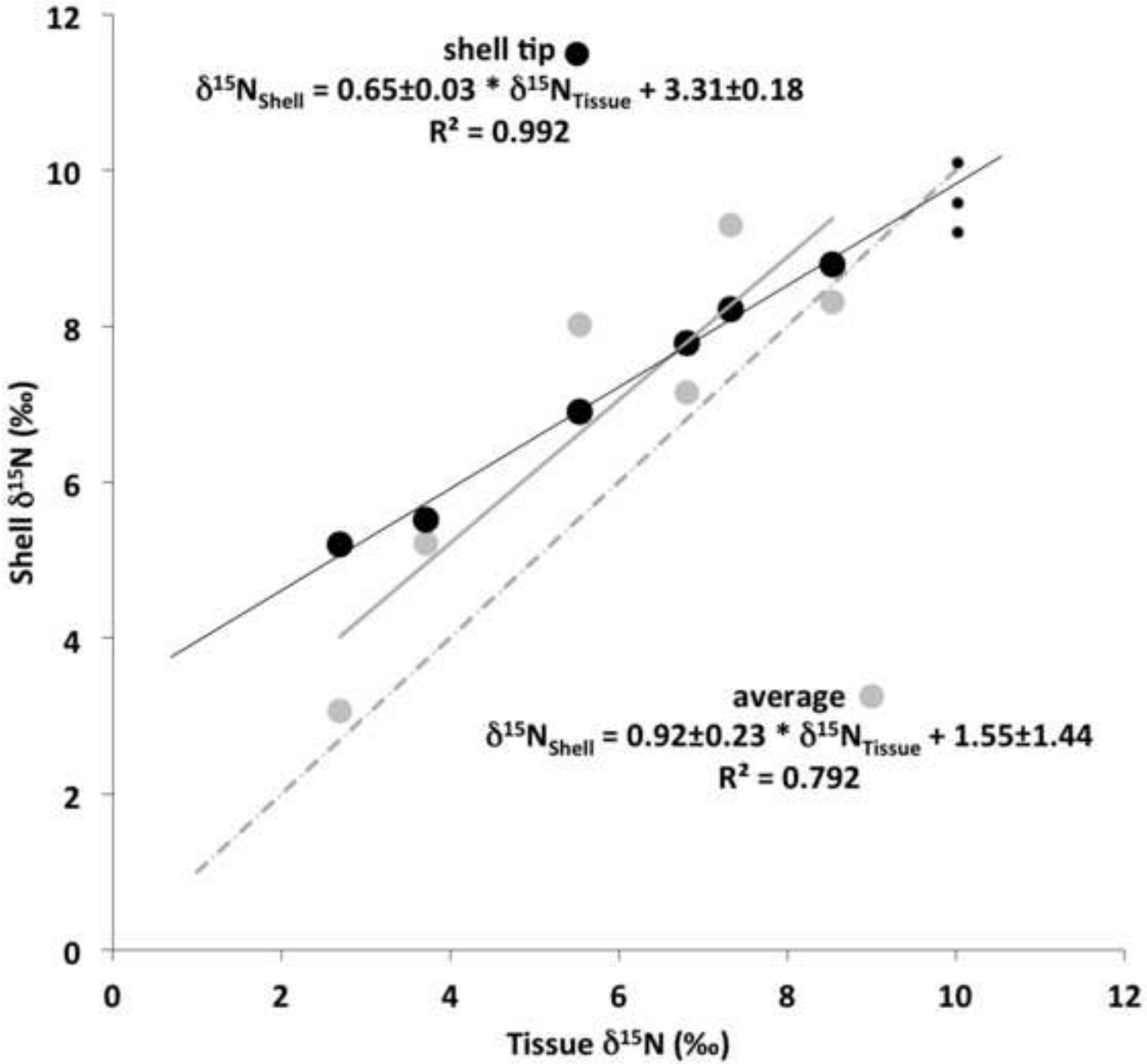
shell tip
$\delta^{15}N_{Shell} = 0.65\pm0.03 * \delta^{15}N_{Tissue} + 3.31\pm0.18$
$R^2 = 0.992$
average
$\delta^{15}N_{Shell} = 0.92\pm0.23 * \delta^{15}N_{Tissue} + 1.55\pm1.44$
$R^2 = 0.792$
Shell $\delta^{15}N$ (‰)
Tissue $\delta^{15}N$ (‰)
0
2
4
6
8
10
12

Figure 8

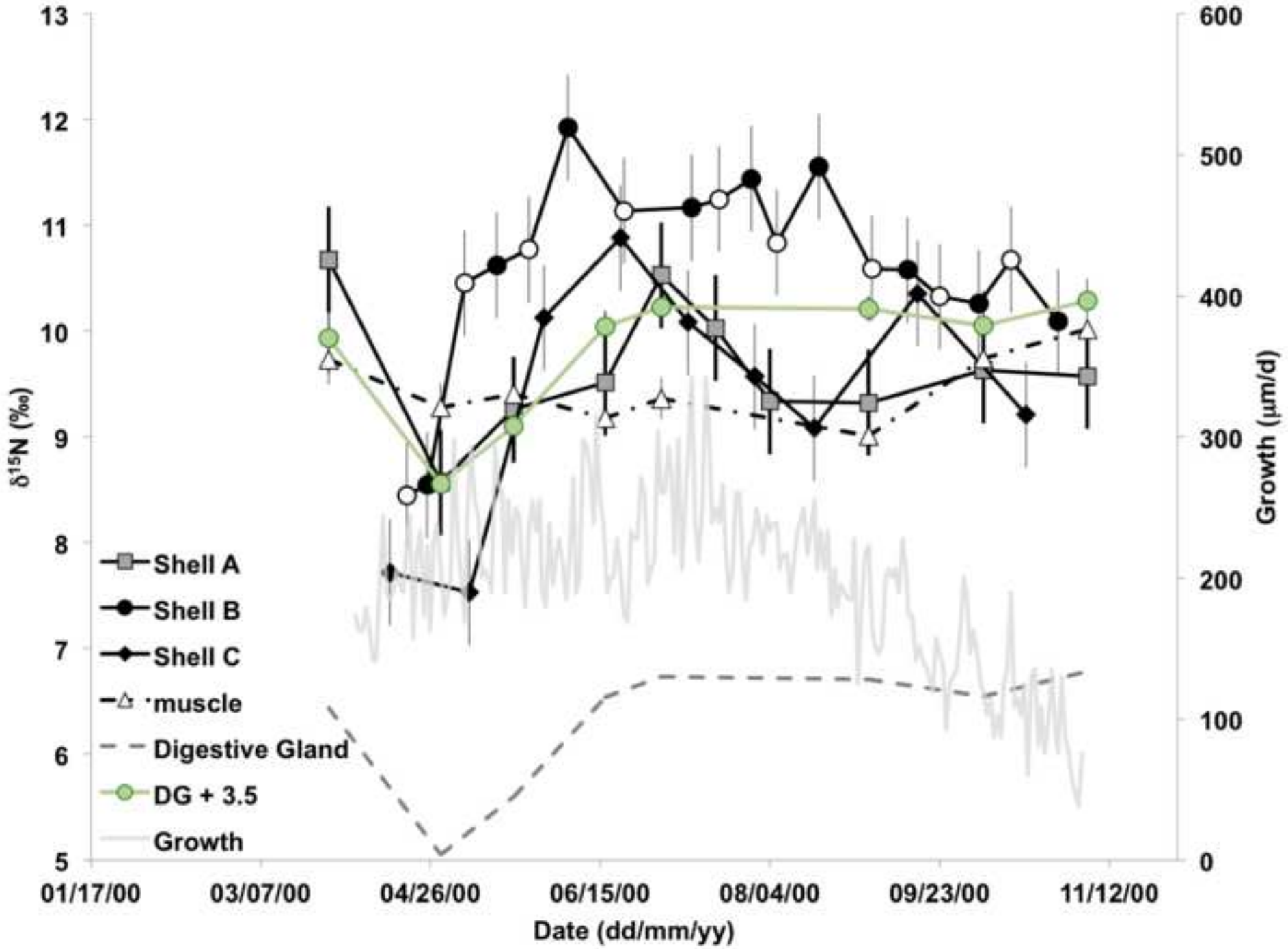
13
12
11
10
9
8
7
6
5
δ15N (‰)
600
500
400
300
200
100
0
Growth (µm/d)
Shell A
Shell B
Shell C
muscle
Digestive Gland
DG + 3.5
Growth
01/17/00
03/07/00
04/26/00
06/15/00
08/04/00
09/23/00
11/12/00
Date (dd/mm/yy)

Figure 9